Hindawi
Advances in Materials Science and Engineering
Volume 2019, Article ID 7029471, 9 pages
https://doi.org/10.1155/2019/7029471

Research Article

Surface Laser Processing of Additive Manufactured 1.2709 Steel Parts: Preliminary Study

O. Černašėjus[1], **J. Škamat**[2], **V. Markovič**[1], **N. Višniakov**[3] and **S. Indrišiūnas**[4]

[1]*Department of Mechanics and Materials Engineering, Vilnius Gediminas Technical University, Vilnius LT-10223, Lithuania*
[2]*Laboratory of Composite Materials, Vilnius Gediminas Technical University, Vilnius LT-10223, Lithuania*
[3]*Laboratory of Materials Research, Vilnius Gediminas Technical University, Vilnius LT-10223, Lithuania*
[4]*Center for Physical Science and Technology, Vilnius LT-02300, Lithuania*

Correspondence should be addressed to O. Černašėjus; olegas.cernasejus@vgtu.lt

Received 1 December 2018; Revised 22 January 2019; Accepted 28 February 2019; Published 1 April 2019

Academic Editor: Akihiko Kimura

Recently, metal selective laser sintering (SLS) techniques have attracted lively interest as a promising technology, which offers a number of unique applications in manufacturing of metal parts with complex internal structure and geometry. However, unsatisfactory surface properties of as-manufactured SLS parts cause high cost of finish processing and restrict wider application of SLS products. The paper presents results of the study, which was taken to evaluate capability of laser processing to improve surface quality of SLS parts manufactured from powder maraging steel 1.2709 (X3NiCoMoTi 18-9-5). The properties of processed surfaces were assessed, and the main dependencies of the roughness, hardness, wear resistance, and phase composition on the main parameters of laser processing—scanning speed, laser power, and number of processing times—were determined. The roughness of surfaces was diminished up to ~41%, the hardness was increased up to ~88%, and the wear resistance was improved up to almost 4 times, as compared with surface of as-manufactured SLS part. The preliminary study has demonstrated that laser processing has considerable potential for improvement of surface conditions of steel additive manufactured parts.

1. Introduction

SLS is one of the additive manufacturing (AM) techniques, which uses a high powered laser to fuse small particles of plastic, metal, ceramic, metal matrix composites, or glass. The laser selectively fuses powdered material by scanning cross sections generated from a 3D digital description of the part. During the build cycle, the platform on which the build is repositioned lowers by one layer. The process continues until the build or model is completed [1].

Using metal SLS technology, also known as laser powder bed (LPB), laser powder bed fusion, or selective laser melting (SLM), it is possible to produce dense metallic parts with complex geometries, internal structures, and functionally graded properties [2–4]. The manufacturing of moulds for industry of plastic products is one of the fields where SLS is considered a valuable technique enabling significant increase in production rates. In contrast to the conventional cast, the SLS allows to produce moulds with complex internal cooling channels located very close to the surface and providing up to 25% reduction of cast cycle. After SLS manufacturing, the mould is thermally treated to obtain acceptable mechanical properties. The surface of as-manufactured part is normally very rough, porous, and sometimes contains nonmetal inclusions and other defects. Therefore, the SLS parts are manufactured with quite big tolerances, and then the surface of the part is mechanically processed to reduce the roughness, remove defected layer, and provide suitable geometry and dimensions. Normally, mechanical processing is carried out in several steps and takes a long time. The particular optimisation of SLS parameters could contribute to improvement of surface conditions of as-manufactured

parts and reduce postprocessing cost. The corresponding studies are being carried out now. The other possible way could be processing of the surface using concentrated heat sources enabling modification of the surface such as laser processing. It is known that laser processing is a flexible method, which induces melting and/or ablation of the metals surface. During melting, the relocation of material, being in liquid state, takes place, resulting in surface smoothing. Using ablation mode, material evaporates, sublimates, or is converted to plasma; defected layer could be removed from the surface of AM-manufactured part in such a way. According to results published by other researches [5–8], laser processing of AM products diminishes significantly their roughness, increases microhardness and wear resistance, seals porosity, refines microstructure, and improves micromachinability. The above named effects were obtained on AM parts produced out of various alloys such as Fe–Co, CoCr, Ti–6Al–4V, TiC11, Inconel 718, bronze, and AISI 420 stainless steel. Laser processing of materials is based on the phenomenon of laser light absorption by material and transformation into heat. The part of laser radiation is reflected from the surface, and what amount of laser light will be absorbed and transformed into heat depends on the number of factors, such as energy parameters of laser beam, physical properties of part material, surface chemical composition and topography, size of the processed part, processing parameters, etc. Therefore, it is too difficult to predict success of the processing for certain product on the basis of results obtained on other material with other surface properties. For AM-manufactured parts, surface condition predetermined by the peculiarities of the sintering technology applied can often be a determining factor in whether a process will be successful for a particular material under certain circumstances or not. To the best of authors' knowledge, at the moment, there are no data on the laser surface processing of AM-manufactured parts produced from maraging steels. The present work had the aim to evaluate effectiveness of laser processing for improvement of surface quality of steel moulds manufactured by metal SLS method from maraging steel typical for these products. The morphology and phase composition, roughness, and microhardness of laser-processed SLS side-on surfaces were analyzed. The wear resistance and tribological properties of the processed surfaces were evaluated as well. These data may be useful for other AM products produced from maraging steels, for which the tribology of surface is highly important. The results are presented below.

2. Materials and Methods

For SLS manufacturing of specimens, steel 1.2709 (0.03% C; < 0.1% Si; < 0.1% Mn; (17–19)% Ni; 4.8% Mo; < 0.8% Ti; (8.5–9.5)% Co; < 0.1% Al; Fe-balance) powder of fraction 7–30 μm was used. At the moment, this steel is one of the most widely used steel grades for SLS-manufactured moulds for plastic casting Figure 1 shows the powder morphology.

The square prism samples with dimensions $15 \times 15 \times 10$ mm were produced by metal SLS process using *Concept Laser M3* equipment. The main laser characteristics and

Figure 1: Morphology of powder used for SLS manufacturing.

sintering parameters are listed in Table 1. The SLS process having finished the samples was separated from the substrate using electric discharge equipment *Charmille cut 200*. Then, the samples were cleaned in ultrasonic bath in C_3H_8O solution at 40°C temperature for 15 min. On-side surfaces of as-sintered samples (shown in Figure 2) were processed using nanosecond pulsed laser *Baltic HP* (crystal matrix YVO_4; Nd; wave length: 1064 nm; power: 20 W; pulse frequency: 100 kHz; pulse duration: 10 ns). Each surface was fully scanned by laser once under various laser powers (2, 2.5, and 3 W) and scanning speeds (1, 2.5, and 5 mm/s); the spot size was 25 μm; the step between adjacent laser passes was 18 μm providing appropriate overlapping. Additionally, three series of samples were prepared applying surface laser processing repeatedly 2, 4, and 6 times. The coding of sample series is given in Table 2.

It is known [9] that during the interaction of laser with solids, three main processes occur: heating of material, its melting, and vaporization. The nature of process happened is largely determined by the energy density E, which can be calculated as follows:

$$E = \frac{P + 0.7P}{V \cdot d} = 1.7\frac{P}{V \cdot d}, \quad (1)$$

where P is the power of laser beam, W; $0.7P$ is the power of adjacent previously scanned laser pass, W; d is the diameter of laser spot (cm); V is the scanning speed (cm/s).

Here, equation (1) evaluates additional energy amount from the previously scanned laser pass. The calculated E values are listed in Table 3. It was observed that E values vary significantly with the variation of P and V and are determined mainly by the scanning speed V. All the values calculated were grouped into three energy levels: El (from ~2,700 to ~4,100 J/cm^2), E2 (from ~5,400 to ~8,200 J/cm^2), and E3 (from 13,600 to 20,400 J/cm^2), E3 being the highest energy level.

The morphology of surfaces and elemental composition of surface layers were analyzed by scanning electron microscopy using JEOL JSM-7600F scanning electron microscope (SEM) coupled with energy dispersive spectrometer (EDS) IncaEnergy 350 (Oxford Instruments) for X-ray microanalysis.

The phase composition of the surfaces obtained was examined by the X-ray diffraction (XRD) technique, using a

Table 1: Characteristics of SLS laser and sintering parameters.

Laser			Thickness of layer, mm	Sintering rate, mm/s	Shielding gas	
Wave length, nm	Power, W	Spot size, mm			Type	Consumption, l/h
1064	100	Ø 0.2	0.03	0.2	Ar	0.75

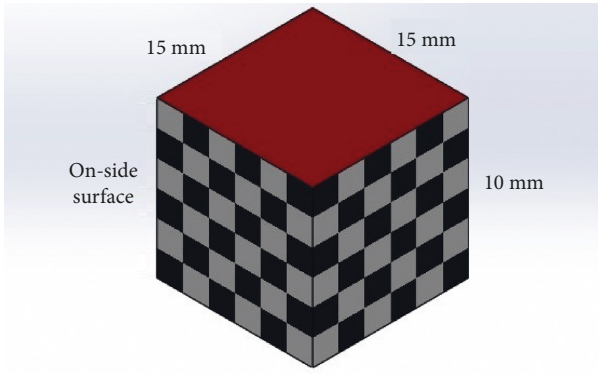

Figure 2: Schematic of SLS sample.

Table 2: Coding of laser-processed samples.

Sample	Parameters of laser processing			
	Laser power P, W	Scanning speed V, mm/s	Number of processing times n	Level of energy input
C1	2	1	1	E3
C2	2	2.5	1	E2
C3	2	5	1	E1
C4	2.5	1	1	E3
C5	2.5	2.5	1	E2
C6	2.5	5	1	E1
C7	3	1	1	E3
C8	3	2.5	1	E2
C9	3	5	1	E1
C10	2.5	2.5	2	E2
C11	2.5	2.5	4	E2
C12	2.5	2.5	6	E2

Table 3: Calculated energy density (J/cm^2).

Scanning speed V, mm/s	Laser power P, W			Level of energy input
	2	2.5	3	
1	13600	17000	20400	E3
2,5	5440	6800	8160	E2
5	2720	3400	4080	E1

BRUKER D8 ADVANCE diffractometer with a Kα (Cu) radiation at a rate of 1°/min and a scanning step of 0.02°. The 2θ scanning was performed in the range between 20° and 80°.

The parameters of surface roughness were determined using the portable profilometer TR-200 with measuring accuracy of ±0.01 μm.

The measurements of microhardness were carried out on prepolished surfaces using the versatile automated hardness tester Zwick Roell ZHμ with measurement error of 1%. The measurements were carried out by Vickers hardness test at the load of 100 g and the exposure time of 10 s. The paper presents values of microhardness calculated as an arithmetic mean of 10 measurements.

The tribology testing was performed by the dry friction test using Microtest tribometer under the following conditions of the experiment: sliding distance: 200 m; sliding speed: 300 rpm; radius of the trajectory: 2 mm; load: 5 N; and temperature of the test: 23°C. "Pin-on-disc" friction scheme was chosen for the experimental test. The indentor was tempered stainless steel cylinder of 3 mm diameter 1.4034. The surface of as-manufactured SLS sample was prepolished before testing ($R_a = 0.2\,\mu$m).

3. Results and Discussion

3.1. Surface Morphology and Roughness. Figure 3 shows the on-side surface morphology of as-manufactured SLS sample. The surface is rough with near-globule shaped and chaotically distributed coarse asperities. The roughness of surface is $R_a = 9.2\,\mu$m. Typical morphologies of surfaces after laser processing at different scanning speed are shown in Figure 4. Three specific morphologies can be pointed out. Not well melted rough cauliflower-like surface morphology (C3, C6, and C9) was obtained under 5 mm/s scanning speed, which corresponds to the lowest E1 energy level. The presence of residues of initial morphology indicates that a part of surface was not laser treated. The reason could be too high "valley-peak" distance and too low energy density. Firstly, at the applied energy level E1, the thickness of material, in which heat is generated, could be less than the "valley-peak" distance; secondly, different microareas of surface are located in different laser focal offset plains, and when the defocusing distance is too high, the energy density can be not enough to melt the material. More uniform, but not well-formed herringbone-like morphology (C2, C5, and C8) was obtained at 2.5 mm/s (E2). The entire surface was treated, and morphology was formed from the individual melt pools generated by the individual laser impulses; however, energy density was, probably, not enough high to provide stable melt pool size under these circumstances. Uniform well-formed herringbone-like morphology (C1; C4; C7) was obtained at 1 mm/s speed (E3), indicating that quite stable and enough deep processing of surface was reached. It is obvious that morphology of surface changes visibly with variation of energy density, and the most uniform surfaces were obtained at the lowest scanning speed (1 mm/s), which corresponds to the highest energy level (E3); no visible changes in morphology were observed with power variation (at constant scanning speed of laser). When surfaces were laser-processed 2, 4,

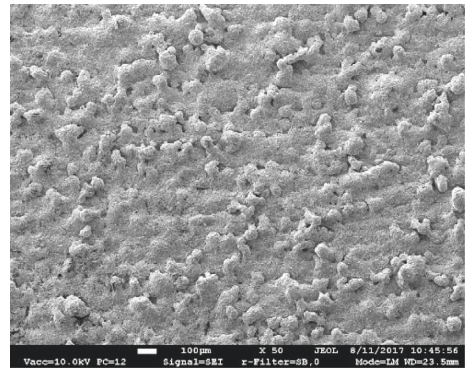

Figure 3: On-side surface morphology of as-sintered SLS sample.

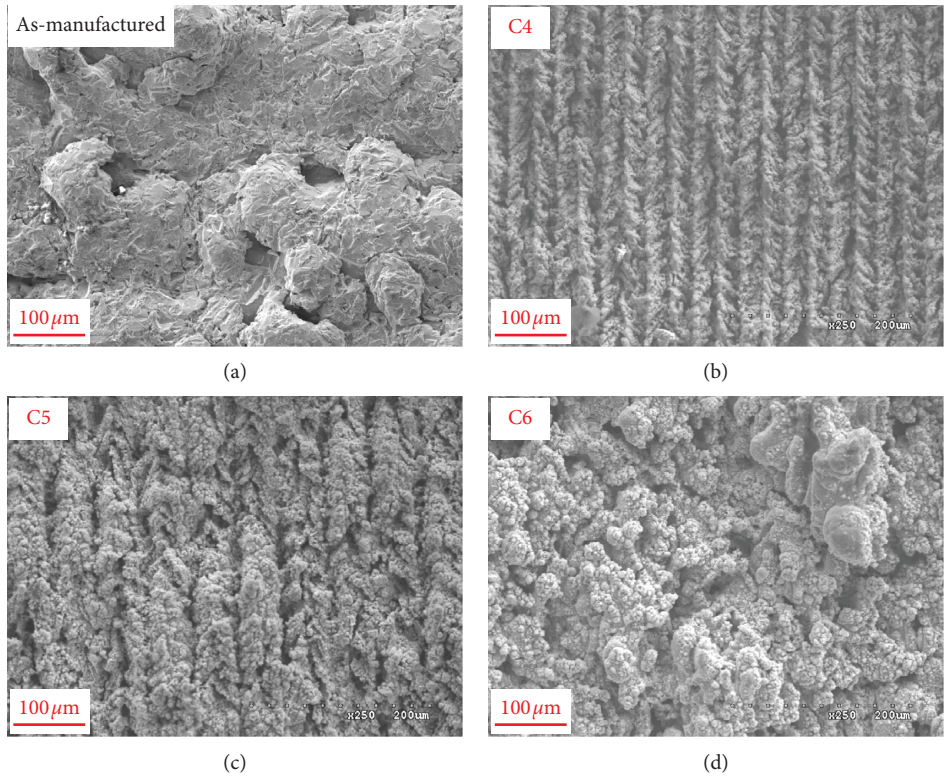

Figure 4: Comparison of as-manufactured surface morphology with morphologies obtained at different scanning speeds and constant power of 2.5 W.

and 6 times, the morphology seemed to become slightly finer and uniform; however, small cracks appeared at $n = 6$ (Figure 5).

The main findings of morphological study were confirmed by the results of roughness measurements (Figures 6 and 7). The roughness of surface obtained at maximum speed ($V = 5$ mm/s) and the lowest power ($P = 2$ W) was $R_a = 8.96\,\mu$m, and it hardly differed from that of the as-manufactured sample ($R_a = 9.2\,\mu$m); however, roughness R_a was reduced significantly while increasing energy density. For the surfaces processed 1, 2, 4, and 6 times, slight gradual reduction of roughness R_a was determined with increase in number of processing times from 1 to 4. The minimum roughness of $R_a = 4.3\,\mu$m was obtained at $n = 4$. Further increase in n up to 6 times resulted in R_a rise associated with formation of cracks.

3.2. Surface Microhardness. The microhardness of laser-processed surfaces was found increased as compared with 297 HV value for as-manufactured SLS surface (Figure 8). The average hardness values for all the laser-processed surfaces ranged from 509 to 558 HV. Clearly, expressed trends of microhardness increase with the decrease in scanning speed and increase in laser power were observed. In general, laser processing allowed to increase hardness

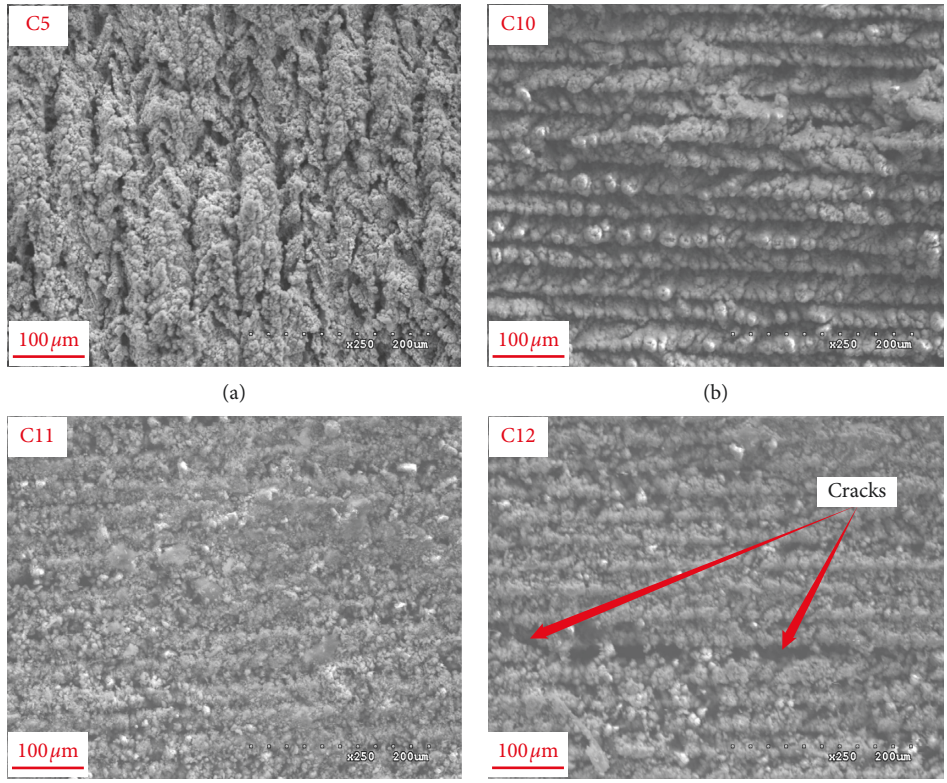

Figure 5: Morphology of surfaces laser-processed 1, 2, 4, and 6 times.

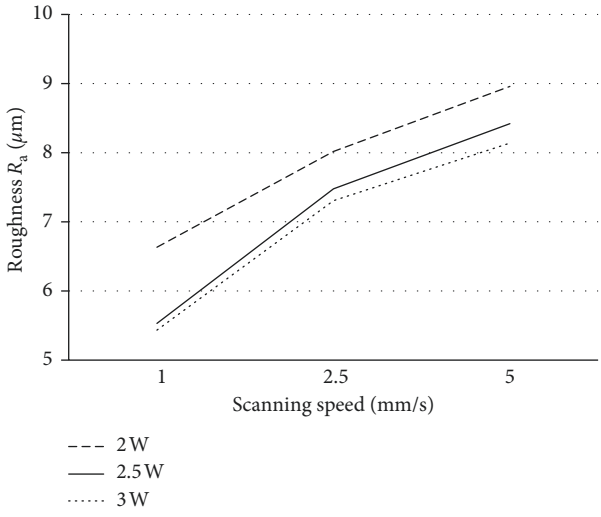

Figure 6: Roughness of laser-processed surfaces.

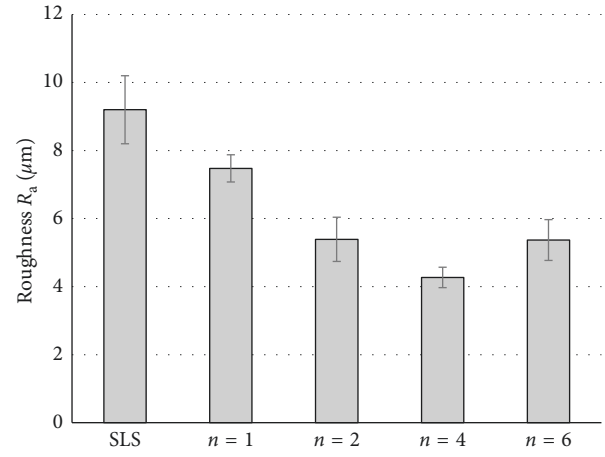

Figure 7: Roughness of surfaces laser-processed 1, 2, 4, and 6 times (2.5 mm/s; 2.5 W). SLS: as-manufactured SLS sample.

from 71% to 88%. The reprocessing of surfaces did not visibly influence hardness of surfaces (Figure 9).

3.3. Surface Tribology. The mass loss of samples determined after dry sliding wear test is presented in Figure 10. The average values ranged between 580 and 2040 μg and were in good correlation with the dependencies obtained for surface roughness and hardness (Figures 6 and 8), providing wear rate reduction from ~5 up to ~73%. According to the Reye–Archard–Khrushchov law [10, 11], the wear rate is reversely proportional to the hardness. It is also well known that wear rate tends to be increased along rise in roughness, since the specific load increases due to reduced real contact area [12]. As was expected, harder and less rough surfaces obtained in this work showed less wear rate. As in the present experiment, harder surfaces were less rough too; the increased wear resistance of laser-processed surfaces is determined by the particular combination of

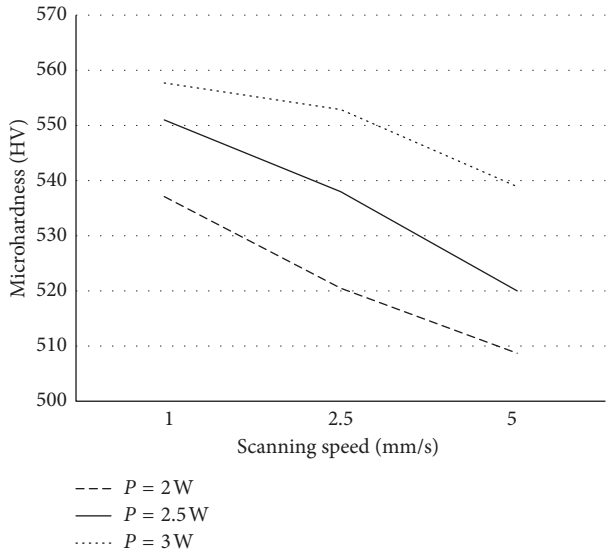

Figure 8: Microhardness of laser-processed surfaces.

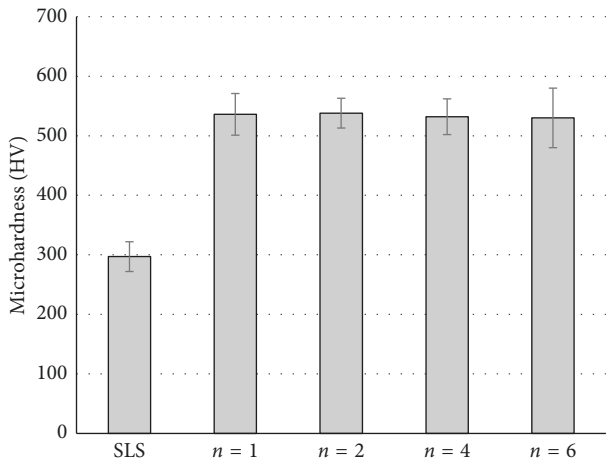

Figure 9: Microhardness of surfaces laser-processed 1, 2, 4, and 6 times (2.5 mm/s; 2.5 W). SLS: as-manufactured SLS sample.

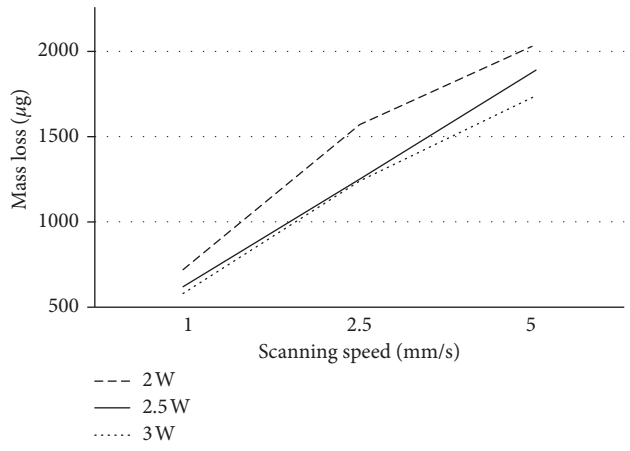

Figure 10: Wear of laser-processed surfaces.

named properties. At the same time, negligible difference was observed between the wear rates of as-manufactured SLS surface (2150 μg) and most rough laser-processed surfaces (1740–2040 μg), obtained at E1 energy level, indicating that roughness, however, could be the dominating factor.

The cracks, surface layer fragmentation, and delamination along with deep scratches, observed on the worn surface of as-manufactured SLS sample, testify the prevalence of delamination and abrasive wear processes (Figure 11(a)). The presence of plastically deformed zones was established as well. A worn surface of laser-processed samples contained mainly craters and debris, indicating that due to higher hardness, laser-processed surfaces can withstand an abrasion much better. That is why the wear loss of laser-processed surfaces was much less. However, due to decreased plasticity, delamination becomes predominant wear mechanism (Figures 5(b)–5(d)). This mechanism seems to be similar for laser-processed samples independently of processing parameters. However, for less rough C4 sample, small amount of fine debris was observed; rougher C5 sample showed much bigger mount of fine debris sample; the most rough C6 sample was characterized by coarse debris. It is believable that mainly, delamination of coarse debris (for C6) and increased amount of fine debris (for C5 sample) causes the significant mass loss.

For surfaces, which were processed 2, 4, and 6 times additionally, significant improvement in wear resistance was achieved (as compared with once laser processed), and the mass loss obtained was in correlation with surface roughness too (Figure 12). The friction coefficient of as-manufactured SLS sample surface was about 1.1 at the steady stage, and according to friction curves obtained (Figure 13), the friction coefficient of surfaces was reduced significantly after laser processing: at the steady stage, it was about 0.7 for once- and twice-processed samples. The lowest and most stable friction coefficient was obtained on surfaces laser-processed 4 times, where the lowest roughness and the best wear resistance were achieved. This finding is in discrepancy with widely known pattern, which says that the lower the roughness is, the bigger the friction coefficient is. Such contradiction indicates that the friction of surfaces in this case was predetermined not by the roughness, but by some other factors, one of which could be the changed phase composition.

3.4. Elemental and Phase Composition of Surface. According to EDS results, the composition of elements of initial powder and SLS surface differed insignificantly; only the slight increase in oxygen content can be pointed out (Table 4). After laser processing, the O concentration at surfaces increased significantly, indicating that intensive oxidation took place during processing. It was also observed that O concentration varies with changing scanning speed. The lower the scanning speed was, the higher the oxygen concentration was observed. This is the result of more prolonged surface interaction with air oxygen due to longer heating and slower cooling rates at lower scanning speed. These results were confirmed by XDR analysis as well. The XRD patterns of as-manufactured SLS sample and samples after laser processing

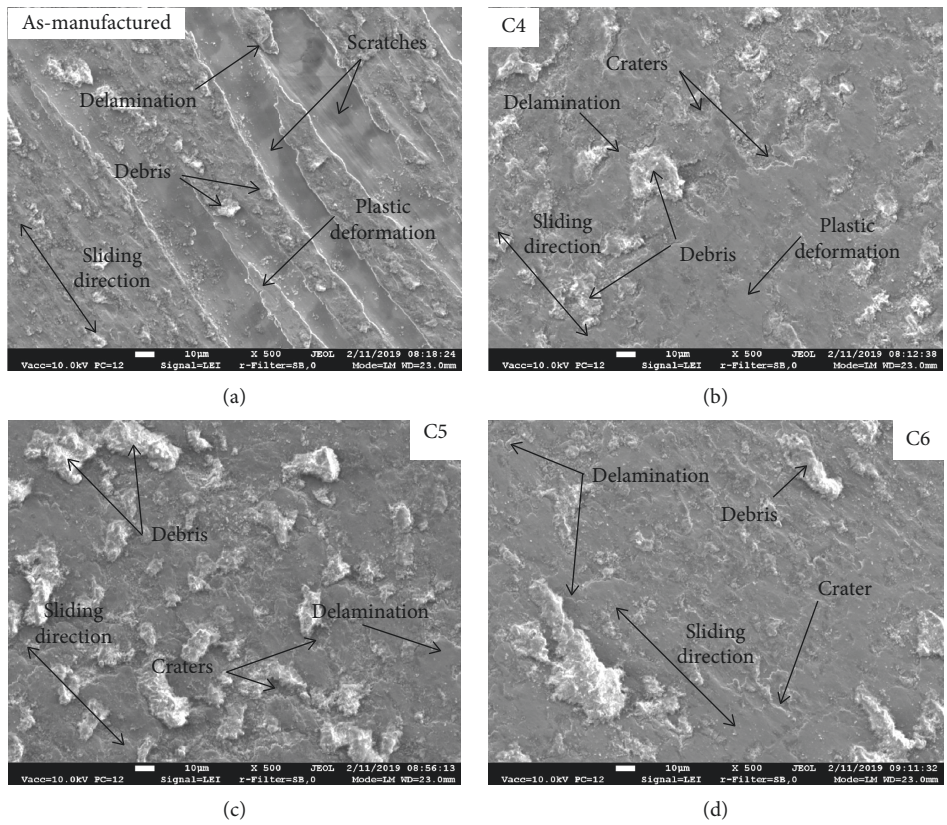

Figure 11: Morphology of the worn surfaces.

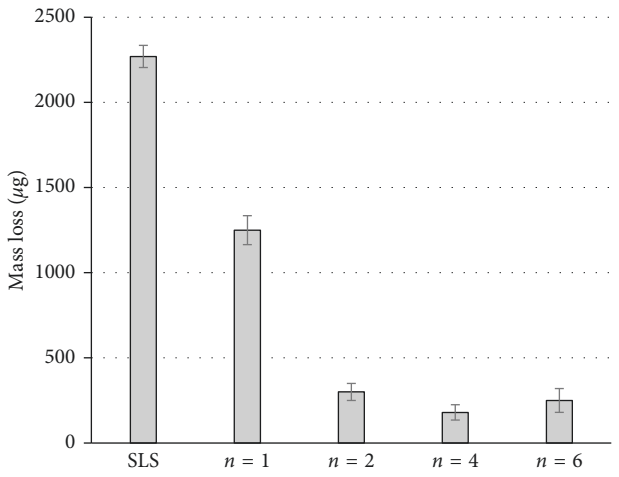

Figure 12: Wear of surfaces laser-processed 1, 2, 4, and 6 times (2.5 mm/s; 2.5 W). SLS: as-manufactured SLS sample.

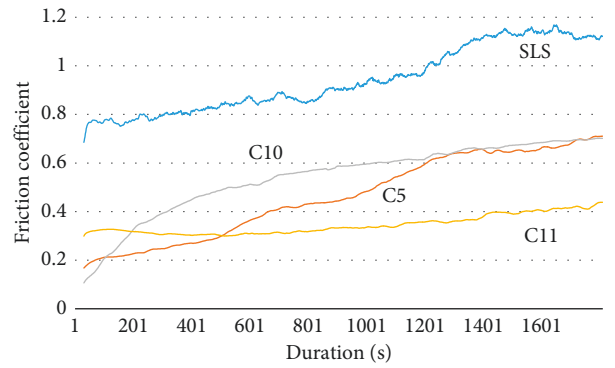

Figure 13: Friction coefficient curves of surfaces laser-processed 1, 2, 4, and 6 times (2.5 mm/s; 2.5 W). SLS: as-manufactured SLS sample.

are shown in Figure 14. The main reflections observed in XRD pattern of SLS sample are attributable to bcc-lattice Fe with parameter $a = 2.866$ Å (Figure 14(a)). This phase can be identified as cubic martensite, which is typical for alloyed steel with low carbon content. Less intensive reflections belong to residual austenite (fcc lattice; $a = 3.63$ Å). At the same time, the presence of intensive reflections attributable to iron cobalt oxide (Fe_2CoO_4) and titanium cobalt oxide ($Ti_{0.11}Co_{0.89}O_{0.99}$) was determined in the XRD patterns of

Table 4: Elemental composition of initial powder and surface of samples (by EDS, in weight%).

Sample	Element					
	Fe	Ni	Co	Mo	Ti	O
Powder for SLS	Balance	20	6.9	4.5	0.7	2.0
As-manufactured SLS sample		23	8.2	4.1	0.7	5.1
C4 (2.5 W/1 mm/s) $n = 1$		14.9	10.6	3.1	1.26	26.0
C5 (2.5 W/2.5 mm/s) $n = 1$		11.8	6.1	4.0	0.8	24.0
C6 (2.5 W/5 mm/s) $n = 1$		10.4	7.6	2.3	0.6	22.1

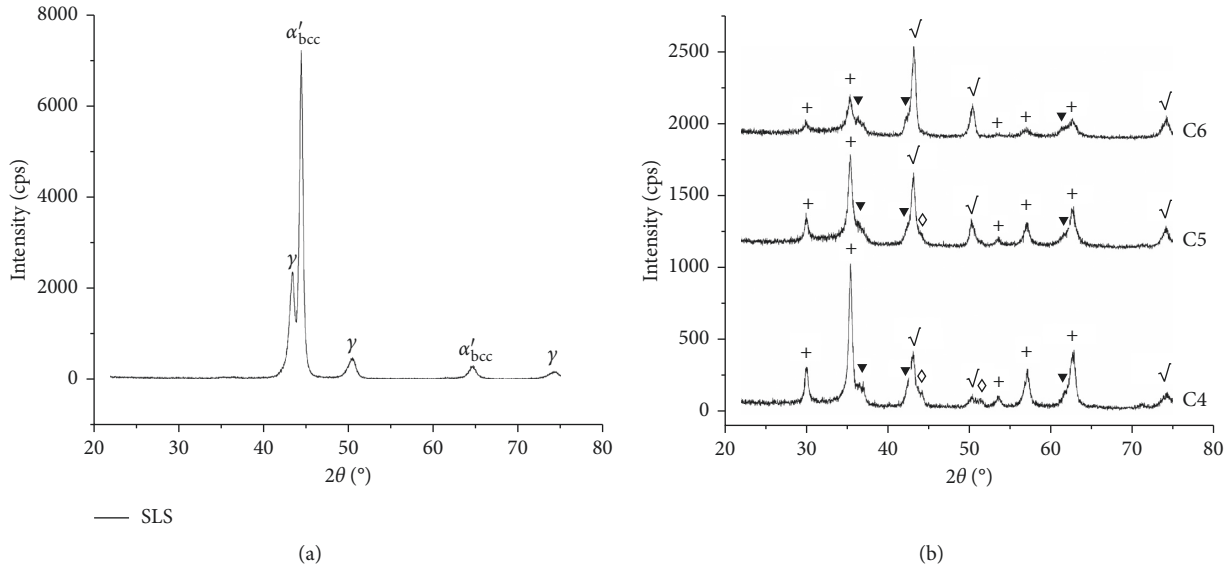

FIGURE 14: XRD patterns of as-manufactured SLS sample (a) and laser-processed samples (b). α'BCC: cubic martensite; γ: austenite; +: Fe_2CoO_4; ▼: $Ti_{0.11}Co_{0.89}O_{0.99}$; √: $Mo_{0.27}Ni_{0.73}$ and/or γ-Fe; ◊: $Mo_{0.03}$ $Ni_{0.97}$ and/or $Fe_{0.5}Ni_{0.5}$.

laser-processed surfaces (Figure 14(b)). Other reflections belong to such phases as $Mo_{0.27}Ni_{0.73}$ ($a = 3.624$ Å) and/or γ-Fe ($a = 3.645$ Å) and $Fe_{0.5}Ni_{0.5}$ ($a = 3.546$ Å) and/or $Mo_{0.03}$ $Ni_{0.97}$ ($a = 3.536$ Å). According to results of Rietveld analysis, the concentration of Fe_2CoO_4 increases with the increase in energy level: 52% of Fe_2CoO_4 was obtained at E1, 64% at E2, and 87% at E3. Such increase can be directly related to longer heating duration and slower cooling rate in air. It should be noted that this trend is in good correlation with results of hardness measurement allowing to assume that the increased surface microhardness is largely predetermined by formation of oxides. Prevalence of oxides at laser-processed surfaces can also explain improvement of friction coefficient.

4. Conclusions

Laser processing was used to improve on-side surface conditions of 1.2709 steel parts produced using additive manufacturing technique, namely, metal SLS. The properties of processed surfaces were evaluated, and dependency of roughness, hardness, wear resistance, and phase composition on the main parameters of laser processing—scanning speed, laser power, and number of processing times—was determined.

It was found that in the case of samples laser processed once, the roughness had tendency to diminish and hardness had tendency to increase when rising the laser power and slowing the scanning speed. The combination of both these properties predetermines significant improvement in wear resistance. The roughness of surfaces was reduced up to ~41%, the hardness was improved up to ~88%, and the wear resistance was improved up to almost 4 times. The most significant effect was obtained at the highest laser power and the slowest scanning speed, corresponding to the highest energy density level E3 applied during the experiment. The obtained results encourage further studies with higher energy densities.

The experiments of laser reprocessing of surfaces 2, 4, and 6 times have shown that repeated processing may help to achieve some improvement of the effect. However, risk of crack occurrence due to overheating should be taken into account.

This preliminary study has demonstrated that the laser processing has the considerable potential for improvement of surface conditions of steel additive manufactured parts.

Data Availability

The tables and figures data used to support the findings of this study are included within the article.

Conflicts of Interest

The authors declare that there are no conflicts of interest regarding the publication of this paper.

References

[1] C. Deckard, "Method and apparatus for producing parts by selective sintering," U.S. Patent 4,863,538, 1989.

[2] L. E. Murr, E. Martinez, S. M. Gaytan et al., "Microstructural architecture, microstructures, and mechanical properties for a nickel-base superal-loy fabricated by electron beam melting," *Metallurgical and Materials Transactions A*, vol. 42, no. 11, pp. 3491–3508, 2011.

[3] D. D. Gu, W. Meiners, K. Wissenbachm, and R. Poprawe, "Laser additive manufacturing of metallic components: materials, processes and mechanisms," *International Materials Reviews*, vol. 57, no. 3, pp. 133–164, 2012.

[4] I. Gibson, D. Rosen, and B. Stucker, *Additive Manufacturing Technologies*, Springer, New York, NY, USA, 2015.

[5] D. Bhaduria, P. Pencheva, A. Batala et al., "Laser polishing of 3D printed mesoscale components," *Applied Surface Science*, vol. 405, pp. 29–46, 2017.
[6] K. C. Yunga, W. J. Wanga, T. Y. Xiaoa et al., "Laser polishing of additive manufactured CoCr components for controlling their wettability characteristics," *Surface and Coatings Technology*, vol. 351, pp. 89–98, 2018.
[7] C. P. Maa, Y. C. Guana, and W. Zhou, "Laser polishing of additive manufactured Ti alloys," *Optics and Lasers in Engineering*, vol. 93, pp. 171–177, 2017.
[8] F. Zhihao, L. Libin, C. Longfei, and G. Yingchun, "Laser polishing of additive manufactured Superalloy," *Procedia CIRP*, vol. 71, pp. 150–154, 2018.
[9] J. Hu, D. Dang, H. Shen, and Z. Zhang, "A finite element model using multi–layered shell element in laser forming," *Optics and Laser Technology*, vol. 44, no. 4, pp. 1148–1155, 2012.
[10] T. Reye, "Zur theorie der zapfenreibung," *Der Civilingenieur*, vol. 6, pp. 235–255, 1860.
[11] V. L. Popov, *Contact Mechanics and Friction*, Springer, Berlin, Germany, 2010.
[12] R. G. Bayer and J. L. Sirico, "The influence of surface roughness on wear," *Wear*, vol. 35, no. 2, pp. 251–260, 1975.